The role of ambient turbulence in facilitating thermal quench of disruptive plasmas in HL-2A tokamak

Y. C. Li[1*], Y. Xu[1], M. Jiang[2], J. Cheng[1], G. Z. Hao[2], X. Q. Wang[1], Z. B. Shi[2], Yi. Liu[2], J. Q. Xu[2], Y. P. Zhang[2], D. N. Wu[1], J. Huang[1], W. Li[1], H. Zhou[1] and J. R. Shao[1]

[1] Institute of Fusion Science, School of Physical Science and Technology, Southwest Jiaotong University, Chengdu 610031, China

[2] Southwestern Institute of Physics, Chengdu 610041, China

*Email: liyucai@swjtu.edu.cn

Plasma disruption in tokamaks is one of the most serious challenges in fusion researches. Experimental and theoretical studies both reveal that the plasma disruption is usually related to uncontrolled growth of magnetohydrodynamic (MHD) instabilities, followed by thermal and current quenches [1-3]. Recent studies suggest that micro-scale turbulence may play an important role in facilitating macro-scale thermal quench (TQ) and resultant disruption [4-6]. However, the experimental evidence about the impact of ambient turbulence on the dynamic evolution of heat transfer during the TQ is lacking. In the HL-2A tokamak, two sorts of disruptive discharges (one has a small temperature collapse before the TQ, while the other has not) have been identified. The results of both types show general tendency that the plasma turbulence is substantially enhanced prior to the TQ [6]. Figure 1 shows typical temporal sequences of plasma parameters across the TQ in a partial disruptive shot. Prior to TQ, it is noticed that there is a sharp rise in the $\dot{B}_\theta$ signal (see blue curve in Fig. 1(d)), which reflects essentially the distortion of magnetic topology before the temperature collapse. The turbulence powers of magnetic fluctuations ($\tilde{B}_\theta^2$) and electron temperature fluctuations ($\tilde{T}_e^2$ detected by ECEI nearby the energy release spot) are plotted in Figs. 1(d) and (e), respectively. One can clearly see that both $\tilde{B}_\theta^2$ and $\tilde{T}_e^2$ abruptly increase ahead of the TQ. These results show explicit evidence that plasma turbulence may play an essential role in facilitating the TQ. In order to investigate the dynamic evolution of the heat transfer and its intriguing interaction with turbulence across the TQ, we analyzed the MHD instability and heat transfer characteristics by scrutinizing the variations of the temperature perturbation and the heat flow pattern captured by the 2D electron cyclotron emission imaging (ECEI), which simultaneously measured the macro-scale electron temperature perturbation (δT_e) and micro-scale temperature fluctuations ($\tilde{T}_e$) [7]. Figure 2(a) shows time traces of $\delta T_e/\bar{T}_e$ (measured by ECEI at R = 184.2 cm and Z = −3.4 cm) and the core electron temperature T_{e0}. The top graphs in Fig. 2(b) illustrate the progressive ECE images (1→3) before the TQ. The images exhibit that an initial heat punctures via the island X-point, and massive energy flows out subsequently. Meanwhile, the magnetic topology is changed significantly. To survey the influence of turbulence on the heat transfer

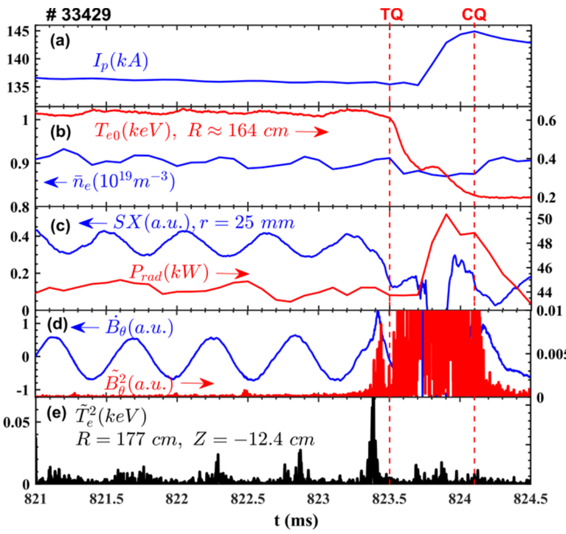

Fig. 1. (a) Plasma current (I_p); (b) core electron temperature (T_{e0}) measured by the ECE and central line-averaged density ($\bar{n}_e$); (c) soft X-ray radiation (SX) and total radiated power (P_{rad}); (d) the magnetic oscillation ($\dot{B}_\theta$) and its fluctuation power ($\tilde{B}_\theta^2$) in the frequency range of 15−200 kHz measured by Mirnov coil and (e) electron temperature fluctuation power ($\tilde{T}_e^2$) in the frequency range of 15−100 kHz measured by ECEI.

via the X-point, we have compared the dynamic evolution of turbulence characters (e.g., propagation and correlation lengths) and their interplay with heat transfer in the above period. The middle graphs in Fig. 2(b) display contour-plots of cross-correlation function (CCF) of $\tilde{T}_e$ measured by ECEI pixels (see the horizontal white line in ECE images). It shows that there exists a clear radially outward propagation in temperature fluctuations. The radial range of the turbulence outward propagation extends for about 10 cm with a phase velocity $\tilde{V}_{r,p} \approx 5\ km/s$. The bottom graphs in Fig. 2(b) indicate that both horizontal (L_{cR}) and vertical (L_{cZ}) correlation lengths gradually increase prior to TQ.

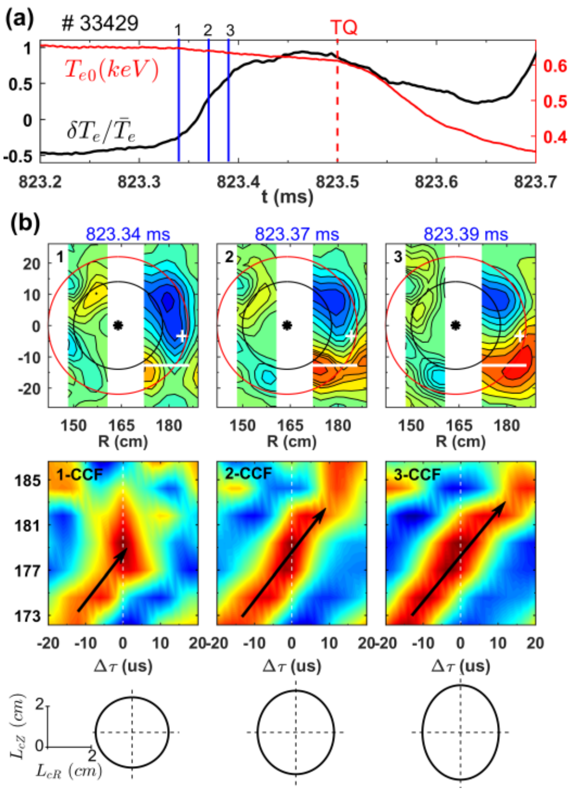

Fig. 2. (a) Time evolutions of T_{e0} and $\delta T_e/\bar{T}_e$ measured at R = 184.2 cm and Z = −3.4 cm (see white cross in Fig. 2 (b)); (b)top: ECE images taken at 3 time points marked by blue vertical lines in (a), the 'asterisk' denotes the axis location, and the black and red circles are q = 1 and q = 2 flux surfaces, respectively; middle: contour-plots of CCF of $\tilde{T}_e$ as a function of time delay ($\Delta\tau$) at the above 3 time points (1→3); bottom: horizontal (L_{cR}) and vertical (L_{cZ}) correlation lengths of turbulence eddies.

For further assessing the energy transfer of turbulence in that duration, the group velocity of turbulence propagation ($\tilde{V}_{r,g}$) has also been estimated by computing the CCF on the envelope of temperature fluctuations. A representative contour-plot of $\tilde{V}_{r,g}$ at $t \approx 823.39\ ms$ (time point 3 in Fig. 2) is depicted in Fig. 3. It is shown that the magnitudes of $\tilde{V}_{r,g}$ inside and near (or outside) the q = 2 surface (at R ≈178 cm) are a bit different. The turbulence energy conveys faster inside ($\tilde{V}_{r,g} \approx$ 3 km/s) than outside ($\tilde{V}_{r,g} \approx$ 1 km/s) when the heat transfer zone becomes broader outside the q = 2 surface, as illustrated in the ECEIs in Fig. 2(b).

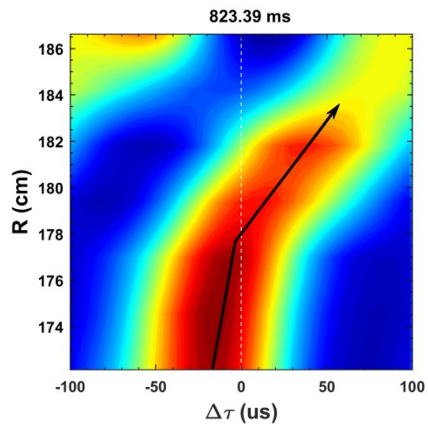

Fig. 3. Contour-plot of CCF on the envelope of $\tilde{T}_e$ measured by ECEI pixel-array (see the horizontal white line in ECE images) as a function of time delay ($\Delta\tau$) at $t \approx 823.39\ ms$.

The above results clearly point out that the ambient turbulence plays a vital role in facilitating thermal quench and subsequent disruption, and provide new insights of the impact of small-scale turbulence on large-scale MHD and disruption events.

References:

[1] N. R. Sauthoff, et al., Nucl. Fusion, **18** 1445, (1978).
[2] T. Hender, et al., Nucl. Fusion **47** S128, (2007).
[3] D. A. Gates, et al., Phys. Rev. Lett. **108** 165004 (2012).
[4] A. Boileau, et al., Nucl. Fusion, **27** 109, (1987).
[5] M. J. Choi, et al., Nat. Commun., **12** 375, (2021).
[6] Y. Li, et al., Sci. Rep. **13** 4785, (2023).
[7] M. Jiang, et al., Rev. Sci. Instruments, **86** 076107, (2015).